Experimental investigation of an Autler-Townes resonator with flow

Yves Aurégan

▶ **To cite this version:**

Yves Aurégan. Experimental investigation of an Autler-Townes resonator with flow. Acta Acustica, 2024, 8, pp.10. 10.1051/aacus/2023065 . hal-04615951

HAL Id: hal-04615951
https://hal.science/hal-04615951v1

Submitted on 18 Jun 2024

HAL is a multi-disciplinary open access archive for the deposit and dissemination of scientific research documents, whether they are published or not. The documents may come from teaching and research institutions in France or abroad, or from public or private research centers.

L'archive ouverte pluridisciplinaire **HAL**, est destinée au dépôt et à la diffusion de documents scientifiques de niveau recherche, publiés ou non, émanant des établissements d'enseignement et de recherche français ou étrangers, des laboratoires publics ou privés.

Public Domain

Acta Acustica 2024, **8**, 10
© The Author(s), Published by EDP Sciences, 2024
https://doi.org/10.1051/aacus/2023065

Available online at:
https://acta-acustica.edpsciences.org

SCIENTIFIC ARTICLE OPEN ACCESS

Experimental investigation of an Autler-Townes resonator with flow

Yves Aurégan*

Laboratoire d'Acoustique de l'Université du Mans, UMR 6613, CNRS, Le Mans Université, Avenue Olivier Messiaen, 72085 Le Mans, France

Received 11 July 2023, Accepted 6 December 2023

Abstract – The acoustic behavior of a double annular resonator with flow is studied as a special case to illustrate the possibilities, but also the difficulties, offered by flow on the acoustic performance of metamaterials. Compared with the associated single resonator, the double resonator exhibits – in the lossless case – a transmission peak near the resonant frequency. This peak is associated with an evanescent out-of-phase coupling between the two resonators and is known in literature as "Autler-Townes splitting". In measurements with a double resonator, this peak is strongly attenuated by viscous effects, to such an extent that it almost disappears. When a flow is added, even a very small one, a gain is created and the peak reappears close to the resonator frequency. As the average flow velocity increases, this gain can become sufficiently large for a whistling to appear.

Keywords: Autler-Townes splitting, Flow effect, Duct

1 Introduction

The filtering effect of a Helmholtz resonator at the wall of an acoustic waveguide has been known for a very long time [1, 2]. Furthermore, the effect of a flow in the waveguide in the presence of a resonator has also been widely studied because of the many practical applications of such a device [3–5]. More recently, a variant where two Helmholtz resonators located in the wall has been studied [6–9]. When the two resonators are so close that they are connected by the evanescent field, an analog of Autler-Townes splitting (ATS) phenomenon appears [10]. This creates a window of transparency in a frequency band where sound waves are not supposed to be transmitted. This effect should not be confused with acoustically induced transparency, which is due to the destructive interference of waves propagating in both directions between the two resonators [8, 9, 11]. Many studies on this phenomenon neglect the effects of flow and sometimes the effects of viscosity. The lack of consideration for flow is all the more strange as this type of system is often referred to as a "ventilated barrier" [12, 13].

The present experimental study aims to take viscosity and flow effects into account in a double Helmholtz resonator. First, the ATS phenomenon is introduced, then the effects of viscosity and flow are introduced. Experimentally, a radical change in behavior is observed in the presence of either viscosity or flow. In particular, the flow-induced gain can be so large that whistling occurs. This gain but also this whistling illustrate the new possibilities, but also the difficulties, offered by the use of flow on the acoustic behavior of metamaterials.

2 Double Helmholtz resonator without viscosity or flow

The investigated device is shown in Figure 1 and its dimensions are given in Table 1. It consists of two identical Helmholtz resonators separated by a plate of small thickness s that is connected to two cylindrical waveguides. The plate can be removed to form a single resonator with the same resonant frequency as the previous two resonators. The central hole of the plate has a diameter (31 mm) slightly larger than that of the waveguides in order to reduce the deviation and scattering of the shear layer by the plate. In both cases, the device is geometrically fully symmetric.

The difference in acoustic behavior between a single resonator and a double resonator is illustrated in Figure 2. This figure is the result of a numerical calculation (using COMSOL) without losses on the geometry given in Table 1. A single resonator produces a relatively wide stop band centered on the resonant frequency. The main difference in the case of a double resonator is the appearance of a narrow transparency band near the resonance frequency.

As shown in [9], this double resonator problem is amenable to matched asymptotic expansion where the small parameter is the reduced wavenumber $k \ll 1$ ($k = 2\pi f R_0/c_0$ with f the frequency, c_0 is the speed of sound and R_0 the

*Corresponding author: yves.auregan@unv-lemans.fr

This is an Open Access article distributed under the terms of the Creative Commons Attribution License (https://creativecommons.org/licenses/by/4.0), which permits unrestricted use, distribution, and reproduction in any medium, provided the original work is properly cited.

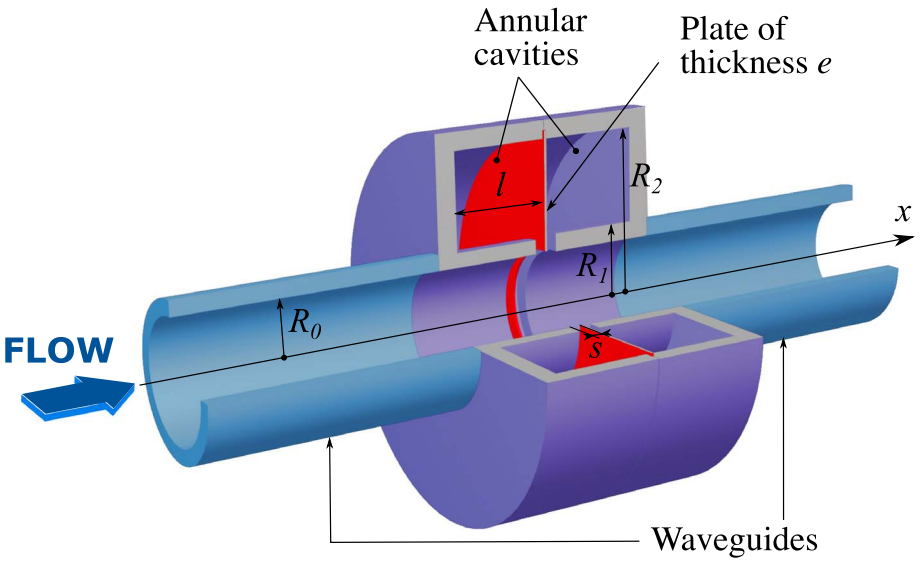

Figure 1. Schematic of the annular double resonator. The flow is considered to be in the positive axial x-direction.

Table 1. Dimensions of the double Helmholtz resonator (see Fig. 1).

	R_0	R_1	R_2	s	e	l
(mm)	15	18	38	2.5	0.5	15

inner radius of cylindrical waveguides that is used to scale any distance). In the outer region (i.e. in the two cylindrical waveguides), only plane wave propagation has to be considered and, without flow, the acoustic propagation can be described by $\nabla^2 p + k^2 p = 0$ where p is the dimensionless pressure scaled by $\rho_0 c_0^2$ and ρ_0 is the density. In the inner region (i.e. in the tube close to the openings of size s of the resonators), the problem to solve is incompressible and it induces jumps in pressure and in velocity for the outer fields.

Due to the complete symmetry of the problem without flow, it can be decomposed into symmetrical and antisymmetrical problems [14] (see Fig. 3). In the symmetrical problems, the pressure is even in x: $p(x, r, f) = p(-x, r, f)$, the axial velocity is odd in x: $u(x, r, f) = -u(-x, r, f)$ while the radial velocity remains even: $v(x, r, f) = v(-x, r, f)$. Conversely, for the antisymmetric solution, $p(x, r, f) = -p(-x, r, f)$, $u(x, r, f) = u(-x, r, f)$ and $v(-x, r, f) = -v(-x, r, f)$.

There is only one symmetric problem (Fig. 3b) that induces an axial velocity jump while the pressure is the same on both sides of the resonator. On the other hand, there are two antisymmetric problems that induce a pressure jump while the axial velocity is the same on both sides of the resonator. In the first antisymmetric case (Fig. 3c), there is no mean velocity entering the resonators. This antisymmetric problem exists whether we are in the case with one or two resonators. Note that this pressure jump is often (but not always [15]) neglected compared to the larger effect of the velocity jump for a single resonator.

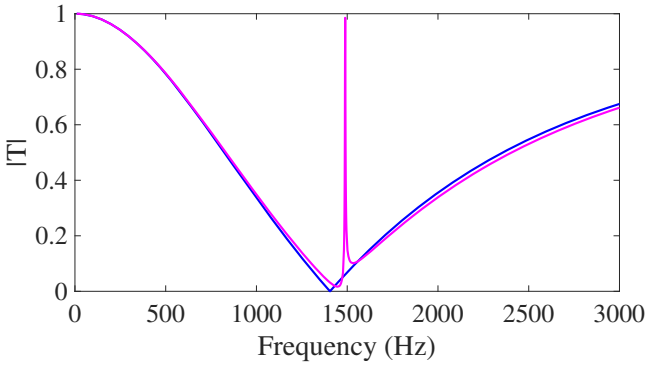

Figure 2. Numerical computation of the transmission coefficient $|T|$ for the single resonator (plate removed, in blue) and for the double resonator (in magenta).

Contrary to the other two solutions this second antisymmetric case (Fig. 3d) exists only when there are two resonators. It corresponds to a motion passing from one resonator to the other. Since there is no average velocity in the waveguides, this motion is only weakly coupled to the waveguides and can be considered a quasi-trapped mode [16].

Following the approach introduced by Porter et al. [9], the effect of both the simple or double resonator can be described by two jumps. One is an axial velocity jump linked to the symmetric problem,

$$[u] = Y_s \bar{p} \tag{1}$$

where $[u] = u_1 - u_2$ where u_1 (resp. u_2) is the outer plane wave axial velocity upstream (resp. downstream) being propagated to the centre of the double resonator ($x = 0$) and $\bar{p} = (p_2 + p_1)/2$ the average pressure in the vicinity of the resonator (p_1 and p_2 are the upstream and downstream outer plane wave pressures at $x = 0$). The second is a pressure jump, linked to the antisymmetric problems,

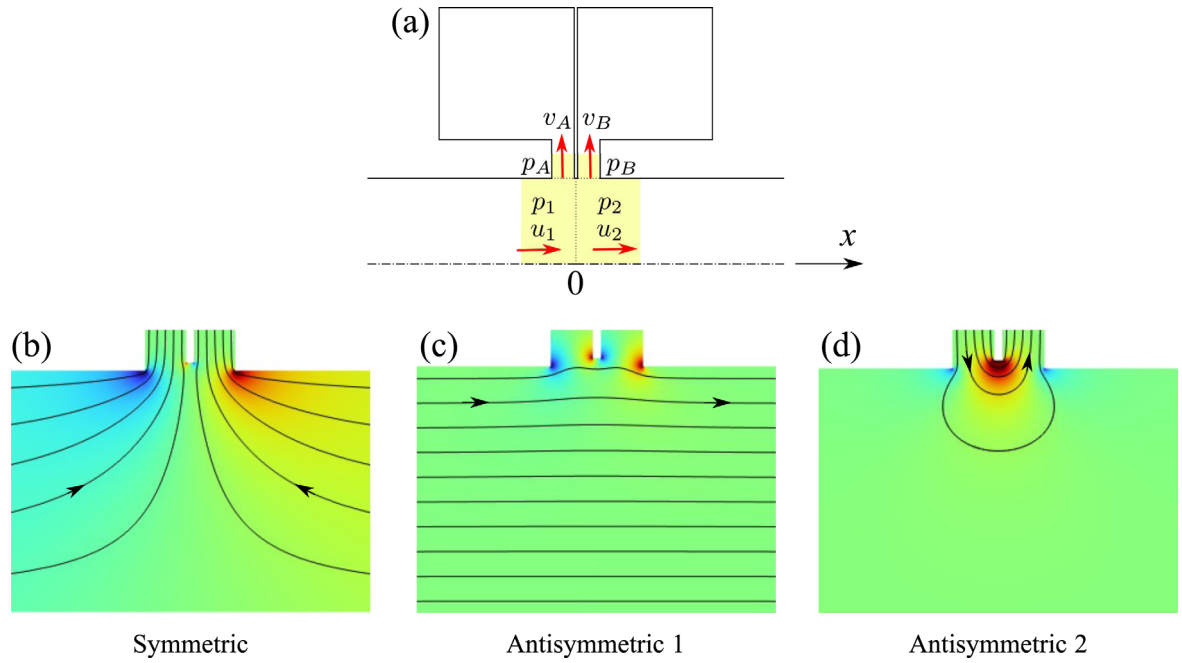

Figure 3. Sketch (a) and numerical simulations of the three incompressible interior problems (b–d). The colors are related to the amplitude of the velocity and the black lines are the stream lines. (b) Symmetric problem. (c) Antisymmetric problem 1 (no mean velocity in the resonators). (d) Antisymmetric problem 2 (no mean velocity in the waveguides).

$$[p] = Z_a \bar{u} \tag{2}$$

only related to the average axial velocity $\bar{u} = (u_2 + u_1)/2$.

From these two jump relations, it is possible to compute the values of the coefficients involved in the velocity and pressure jumps from the transmission coefficients T and reflection R coefficients of this reciprocal and symmetrical device (obtained either numerically or experimentally):

$$Y_{\rm s} = 2\,\frac{1-(T+R)}{1+(T+R)},\; Z_{\rm a} = 2\,\frac{1-(T-R)}{1+(T-R)}. \tag{3}$$

The jump coefficients ($Z_{\rm s} = 1/Y_s$ and $Z_{\rm a}$) numerically obtained on the investigated devices are plotted in Figure 4. A few remarks can be made about these curves. Firstly, as expected, the $Z_{\rm s}$ impedances for the single resonator and the double resonator are very close. The small difference observed at the highest frequencies is due to the small but finite thickness of the plate. On the other hand, the $Z_{\rm a}$ coefficient for the double resonator is very different from the single resonator case. The general behavior (linear and decreasing) of the coefficient is similar to that of the first antisymmetric problem (Fig. 3c; nearly identical to the single-cavity case), but the contribution of the second second antisymmetric problem (Fig. 3d) is significant around the resonance frequency. It was found during the computations that the shape and frequency position of this second contribution is very sensitive to the exact geometry of the intermediate plate (thickness, internal diameter). The transmission peak observed in Figure 2 is at a frequency $f = 1489$ Hz which is very close to the resonance frequency at $Z_{\rm a}$. Note that the frequency of zero impedance for $Z_{\rm s}$ and the frequency of resonance for $Z_{\rm a}$ are slightly different because of the difference in the added mass between these two cases.

3 Experimental results without flow and effect of viscosity

The double resonator described in Figure 1 is mounted between two measuring sections, upstream and downstream. Each measuring section consists of a circular steel tube with rigid walls (inner diameter 30 mm) in which four microphones are mounted. Two acoustic sources on either side of the system produce two different acoustic states and the four elements of the scattering matrix (transmission and reflection coefficient in both directions) for plane waves can thus be evaluated. A more detailed description of the measurement technique can be found in [17, 18]. The measured transmission coefficient of the double resonator is given in green symbols on Figure 5.

The measurement of the double resonator does not show the transparency peak found in the simulation. This quasi-disappearance is due to the viscosity, as demonstrated by the numerical simulation in which thermoviscous effects were taken into account in the resonator necks via the equivalent impedance of the thermo-viscous boundary layer [19] (black line in Fig. 5). So even a very small loss can have a dramatic effect on acoustic behavior (the real part of $Z_{\rm s}$ which gives the losses is experimentally estimated at 0.007 for this device). This is all the more true as the quasi-trapped mode responsible for the transparency peak is poorly coupled to the waveguide, producing a very narrow peak.

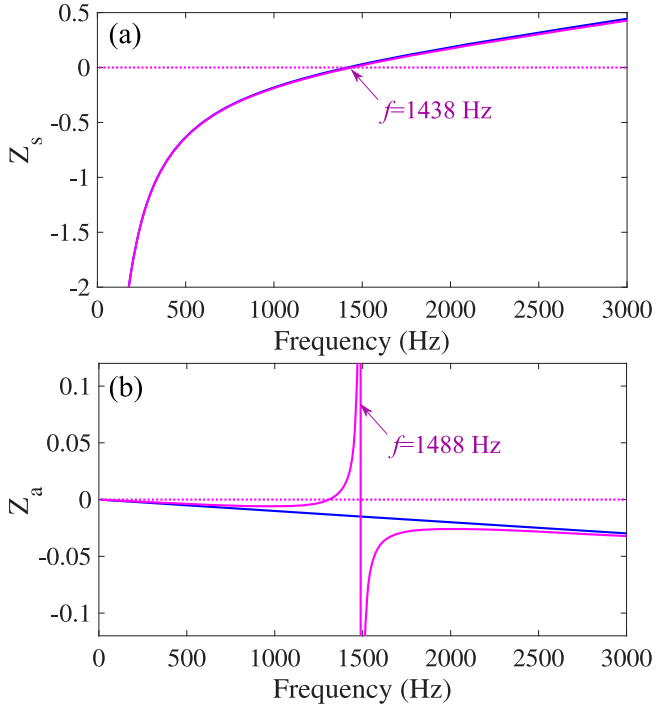

Figure 4. Jump coefficients $Z_s = 1/Y_s$ (a) and Z_a (b) of the single resonator (in blue) and of the double resonator (in magenta). These results are numerically computed in absence of viscosity. Continuous line: imaginary part, dashed line: real part which is equal to 0 without viscosity.

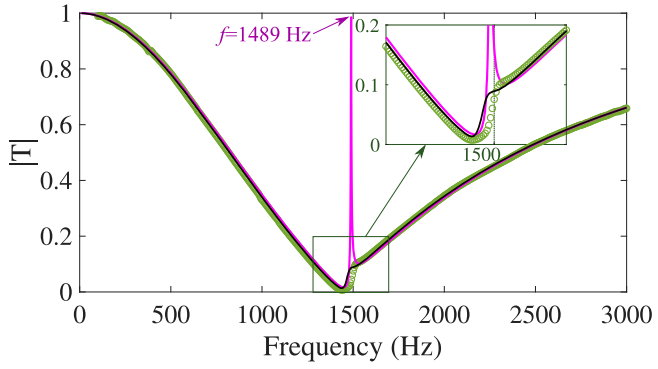

Figure 5. Modulus of the transmission coefficient $|T|$ for the double resonator. Green symbols: experimental results, black line: numerical simulation with losses, magenta line: numerical simulation without losses.

4 Effect of the flow on the double resonator

When an airflow is added into the waveguides and the device, the most remarkable effect is that the double resonator begins to whistle at low velocity values (above 13 ms^{-1}) (see Fig. 6). The frequency of the whistling remains relatively constant and is locked close to the resonance frequency of the resonators. The Strouhal number of appearance of the whistling is given by

$$S_t = \frac{f_R\, s}{U_c} = 0.29 \qquad (4)$$

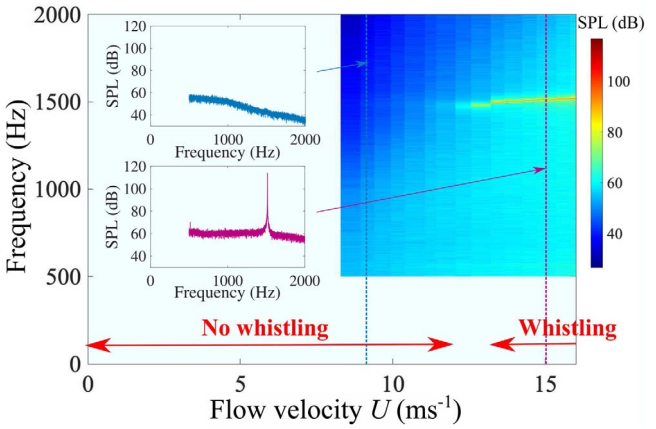

Figure 6. Colormap of the noise level measured in the upstream duct in the presence of flow as a function of flow velocity end frequency. It shows the appearance of a whistling above a flow velocity of 13 ms^{-1}. The two insets are the noise spectrum at 9 and 15 ms^{-1}.

where $f_R = 1500$ Hz is the resonance frequency and $U_c = 13$ ms^{-1} is the critical mean flow velocity where the whistling appears. In contrast, the single resonator, obtained by removing the plate, does not whistle over the whole range of flow velocities studied (up to 30 ms^{-1}).

This whistling is due to the interaction between the acoustic wave and the shear layer created by the flow at the opening of the resonator, which results in an exchange of energy between the flow and the acoustics. This can lead to additional dissipation or energy gain for the acoustics [18, 20, 21]. In the following, only the case without whistling will be studied (the mean flow velocity U is such as $U < U_c$), as the concept of the scattering matrix becomes meaningless when non-linear effects are present, as in the case of whistling. The second noticeable point with flow is that the expected transparency peak (which was not present without flow due to the viscous effects in the neck) appears in the presence of flow (see Fig. 7a). In this figure, note also the difference between downstream propagation (T^+, solid line) and upstream propagation (T^-, dashed line). This difference indicates a loss of reciprocity due to flow. In Figure 7b, the convected reflection coefficients are shown: $R_c^+ = (1-M)R^+/(1+M)$ and $R_c^- = (1+M)R^-/(1-M)$ where R^+ and R^- are the upstream and downstream reflection coefficients where M is the Mach number defined as $M = U/c_0$. The advantage of using the convected reflection coefficients is that they are directly related to energy losses and gains in the system [18, 22]. For example, the fact that R_c^+ and R_c^- are greater than 1 for a certain frequency range in Figure 7b means that the energy of the reflected waves is greater than the energy of the incident waves for that frequency range.

From the scattering coefficients T^+, T^-, R_c^+ and R_c^-, it is possible to construct the convected scattering matrix S_c by

$$\begin{pmatrix} (1+M)p_2^+ \\ (1-M)p_1^- \end{pmatrix} = \mathsf{S}_c \begin{pmatrix} (1+M)p_1^+ \\ (1-M)p_2^- \end{pmatrix}, \text{ where } \mathsf{S}_c = \begin{bmatrix} T^+ & R_c^- \\ R_c^+ & T^- \end{bmatrix} \qquad (5)$$

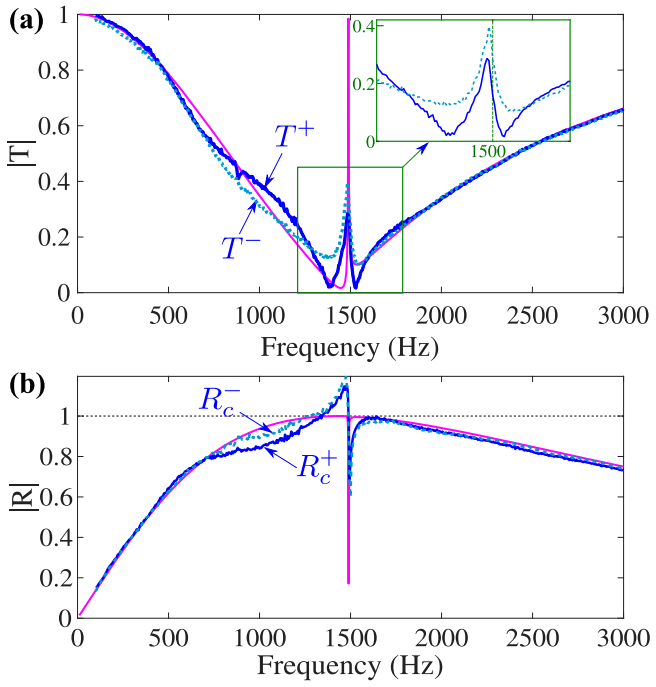

Figure 7. Modulus of the transmission coefficient (a) and of the convected reflection coefficients (b) of the double resonator. Magenta line: Numerical result without viscosity and flow. Blue line: experimental results with flow ($U = 11.5$ ms^{-1}, continuous line in flow direction, dashed line against the flow)

which links scattered waves p_2^+ and p_1^- to the incident waves p_1^+ and p_2^- where the subscript 1 (resp. 2) indicates the upstream (resp. downstream) value of the plane wave being propagated to the center of the double resonator, the superscripts $+$ and $-$ indicate the downstream and upstream propagations. The two eigenvalues of the matrix $\mathsf{I} - \mathsf{S}_c^*\mathsf{S}_c$, where I is the identity matrix and the star stands for the complex conjugate, correspond respectively to the maximum and minimum energy dissipation that is possible in the device divided by the incident energy (a negative value indicates an energy production) [22]. These eigenvalues are computed from the experimental values with and without flow and plotted in Figure 8.

For the double resonator without flow (green lines), the dissipation of the double resonator is between 0 and 5% of the incident energy except for a bump around the resonance frequency where the dissipation is between 5% and 22% of the incident energy.

In the presence of flow for the single resonator (magenta lines), several bumps in attenuation (440 Hz, 1230 Hz) and in gain (890 Hz, 1730 Hz) appear. This is a rather classic behavior resulting from the fact that, depending on the ratio between the length of the aperture and the hydrodynamic wavelength of the disturbance in the shear layer, there is a positive or negative transfer of energy between the acoustic and the flow [23–25]. This ratio is proportional to the Strouhal number given by $S_t = f2s/U$ where U is the mean flow velocity. For the dissipation bump this value is equal to $S_t = 0.17$ and 0.48 and for the gain bumps $S_t = 0.35$ and 0.68.

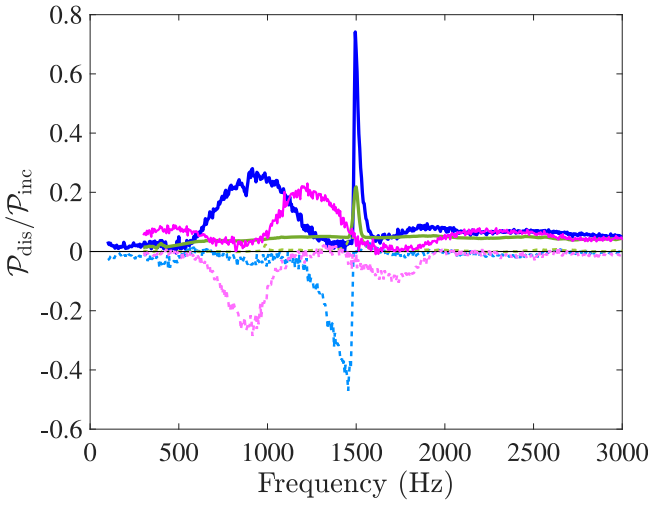

Figure 8. Eigenvalues of the matrix $\mathsf{I} - \mathsf{S}_c^*\mathsf{S}_c$. Double resonator: Green $U = 0$, blue $U = 11.5$ ms^{-1}. Single resonator: magenta $U = 11.5$ ms^{-1}. The solid line is the maximum value, while the dashed line is the minimum value.

For the double resonator at the same flow velocity (blue lines), the first dissipation bump is around 975 Hz showing that the flow allows to dissipate up to 28% of the incident energy. The maximum of this positive bump changes in amplitude and frequency as a function of the mean flow velocity U and the frequency shift of the maximum is such that the Strouhal number $S_t = fs/U = 0.19$ is constant. For higher frequencies, there is a rapid decay of the minimum curve indicating a gain in the double resonator (up to 47%). This gain stops abruptly close to the resonance frequency to produce again an important loss (energy dissipation up to 74%). This narrow-band transition phenomenon, occurring close to the frequency of the transmission peak, is most likely due to the quasi-trapped mode existing in the double resonator.

The description using two jump coefficients, as for the case without flow, derives from the reciprocity and symmetry of the device. In the presence of flow, reciprocity and symmetry are broken and this description can no longer be used. Velocity and pressure jumps then depend on both average pressure and velocity values, and no simple model has been found to explain the measured behavior. Furthermore, for such a geometry, numerical prediction of acoustic behavior with flow is not well predicted by codes using the linearized Euler model. For precise prediction of aeroacoustic behavior, highly accurate but demanding codes are required, such as direct numerical simulation or large eddy simulation [26].

5 Conclusions

When dealing with metamaterials, resonant systems are often used. It is therefore particularly important to take into account the effects of viscosity and flow (if it is appropriated) in sufficient detail. These two effects can significantly alter the expected acoustic effects [27, 28]. In this

paper, this is illustrated by the case of a double Helmholtz resonator. The expected transparency band due to Autler-Townes splitting disappears almost completely in experiments due to viscosity, even though dissipation is rather weak. When a low flow velocity is added, the transparency band reappears experimentally due to the gain generated by the flow. However, at slightly higher flow velocities, a whistling is produced. The gain that occurs in acoustics with flow can be used for some interesting non-Hermitian effects, but it can also lead to difficulties in silencer design, where the potential for whistling can make devices unusable for sound attenuation.

Acknowledgments

The author would like to thank Agnès Maurel, Kim Pham and Joachim Golliard for their fruitful discussions.

Conflict of interest

Author declared no conflict of interests.

Data availability statement

Data are available on request from the authors.

References

1. J.W.S.B. Rayleigh: The theory of sound, Vol 2. Macmillan, 1896.
2. G. Stewart: Influence of a branch line upon acoustic transmission of a conduit. Physical Review 26 (1925) 688–690.
3. J. Anderson: The effect of an air flow on a single side branch Helmholtz resonator in a circular duct. Journal of Sound and Vibration 52 (1977) 423–431.
4. D. Ronneberger: The dynamics of shearing flow over a cavity – A visual study related to the acoustic impedance of small orifices. Journal of Sound and Vibration 71 (1980) 565–581.
5. M.L. Munjal: Acoustics of ducts and mufflers with application to exhaust and ventilation system design. John Wiley & Sons, 1987.
6. A. Santillán, S.I. Bozhevolnyi: Acoustic transparency and slow sound using detuned acoustic resonators, Physical Review B 84 (2011) 064304.
7. A. Merkel, G. Theocharis, O. Richoux, V. Romero-García, V. Pagneux: Control of acoustic absorption in one-dimensional scattering by resonant scatterers. Applied Physics Letters 107 (2015) 244102.
8. Y. Cheng, Y. Jin, Y. Zhou, T. Hao, Y. Li: Distinction of acoustically induced transparency and Autler-Townes splitting by Helmholtz resonators. Physical Review Applied 12 (2019) 044025.
9. R. Porter, K. Pham, A. Maurel: Modeling Autler-Townes splitting and acoustically induced transparency in a waveguide loaded with resonant channels. Physical Review B 105 (2022) 134301.
10. S.H. Autler, C.H. Townes: Stark effect in rapidly varying fields. Physical Review 100 (1955) 703721.
11. T.Y. Abi-Salloum: Electromagnetically induced transparency and Autler-Townes splitting: Two similar but distinct phenomena in two categories of three-level atomic systems, Physical Review A 81, (2010) 053836.
12. H. Nguyen, Q. Wu, X. Xu, H. Chen, S. Tracy, G. Huang: Broadband acoustic silencer with ventilation based on slit-type Helmholtz resonators. Applied Physics Letters 117 (2020) 134103.
13. Y.-X. Gao, Z.-W. Li, B. Liang, J. Yang, J.-C. Cheng: Improving sound absorption via coupling modulation of resonance energy leakage and loss in ventilated metamaterials. Applied Physics Letters 120 (2022) 261701.
14. L. Chesnel, V. Pagneux: Simple examples of perfectly invisible and trapped modes in waveguides. Quarterly Journal of Mechanics and Applied Mathematics 71 (2018) 297–315.
15. V. Dubos, J. Kergomard, A. Khettabi, J.-P. Dalmont, D. Keefe, C. Nederveen: Theory of sound propagation in a duct with a branched tube using modal decomposition. Acta Acustica united with Acustica 85 (1999) 153–169.
16. V. Pagneux, Trapped modes and edge resonances in acoustics and elasticity. In: R.V. Craster, J. Kaplunov, Eds. Dynamic localization phenomena in elasticity, acoustics and electromagnetism. CISM International Centre for Mechanical Sciences, vol. 547, Springer, Vienna, 2013, pp. 181–223.
17. Y. Aurégan, M. Leroux: Failures in the discrete models for flow duct with perforations: an experimental investigation. Journal of Sound and Vibration 265 (2003) 109–121.
18. P. Testud, Y. Aurégan, P. Moussou, A. Hirschberg: The whistling potentiality of an orifice in a confined flow using an energetic criterion. Journal of Sound and Vibration 325 (2009) 769–780.
19. M. Berggren, A. Bernland, D. Noreland: Acoustic boundary layers as boundary conditions. Journal of Computational Physics 371 (2018) 633–650.
20. Y. Aurégan, V. Pagneux: Pt-symmetric scattering in flow duct acoustics. Physical Review Letters 118 (2017) 174301.
21. C. Bourquard, A. Faure-Beaulieu, N. Noiray: Whistling of deep cavities subject to turbulent grazing flow: intermittently unstable aeroacoustic feedback. Journal of Fluid Mechanics 909 (2021) A19.
22. Y. Aurégan, R. Starobinski: Determination of acoustical energy dissipation/production potentiality from the acoustical transfer functions of a multiport. Acta Acustica united with Acustica 85 (1999) 788–792.
23. J. Golliard, N. González-Díez, S. Belfroid, G. Nakiboğlu, A. Hirschberg: U-RANS model for the prediction of the acoustic sound power generated in a whistling corrugated pipe. In: Proceedings of the ASME 2013 Pressure Vessels and Piping Conference, Paris, France. July 14–18 (Paper no. V004T04A040), Vol. 55683. American Society of Mechanical Engineers, 2013, pp. 1–6.
24. J. Golliard, Y. Aurégan, T. Humbert: Experimental study of plane wave propagation in a corrugated pipe: linear regime of acoustic-flow interaction. Journal of Sound and Vibration 472 (2020) 115158.
25. M.E. D'Elia, T. Humbert, Y. Aurégan: Linear investigation of sound-flow interaction along a corrugated plate. Journal of Sound and Vibration 534 (2022) 117048.
26. R. Lacombe, S. Föller, G. Jasor, W. Polifke, Y. Aurégan, P. Moussou: Identification of aero-acoustic scattering matrices from large eddy simulation: Application to whistling orifices in duct. Journal of Sound and Vibration 332 (2013) 5059–5067.
27. Y. Aurégan, M. Farooqui, J.-P. Groby: Low frequency sound attenuation in a flow duct using a thin slow sound material. Journal of the Acoustical Society of America 139 (2016) EL149.
28. M. D'Elia, T. Humbert, Y. Aurégan: Effect of flow on an array of Helmholtz resonators: Is Kevlar a "magic layer"?. Journal of the Acoustical Society of America 148 (2020) 3392–3396.

Cite this article as: Aurégan Y. 2024. Experimental investigation of an Autler-Townes resonator with flow. Acta Acustica, **8**, 10.